Supporting Information

Reineke et al. 10.1073/pnas.1305882110

SI Materials and Methods

Materials. Polystyrene microspheres (MSs) with mean diameters of 500 nm and 1, 2, and 5 μm were purchased from Polysciences and were stored at 4 °C until further use. Suspensions were used as received from the manufacturer (25 mg MS/mL). A dosage volume of 1 mL (total microsphere weight ~ 25 mg) was used in all studies. All of the particles used in the study are part of the carboxylated Polybead product line from Polysciences. They are a series of monodisperse polystyrene MSs that are provided as aqueous suspensions with minimal surfactant in the final preparation. The particles have a slight anionic charge from sulfate ester and have been synthesized to achieve precise size distributions. These particles were selected so that all of the particles would be identical with the exception of particle size for the different study groups.

The uptake inhibitors chlorpromazine (CPZ), phorbol 12-myristate 13-acetate (PMA), cytochalasin B (CytB), and CytD were purchased from Sigma-Aldrich and stored according to the manufacturer's instructions. Dosing concentrations and intervals were selected for each inhibitor by using material safety data sheets and in vitro cell culture protocols published in the literature (1–8). CPZ and colchicine were dissolved into phosphate buffer solution (concentration = 50 μg/mL and 0.1 mM, respectively) immediately before administration. CytB, CytD, and PMA were dissolved into dimethyl sulfoxide and stored at −80 °C until use. Immediately before administration, dimethyl sulfoxide and inhibitor solutions were thawed and diluted in PBS to concentrations of 60, 4, and 2 μM for CytB, CytD, and PMA, respectively.

Isolated Loop Procedure. Male Sprague–Dawley rats (200–250 g) were anesthetized with 3% (vol/vol) isoflurane. After sedation, a 3-cm midline incision was made, and the desired section of the small intestine was identified. The proximal jejunum was located by identifying the ligament of Trietz; the distal jejunum and the beginning of the proximal ileum were located by visualizing an increase in the density of GALT. The distal ileum was identified by locating the cecum. Once the desired sections of the small intestine were identified, a 6-cm segment was isolated with two ligatures that were created using monofilament silk 0-0 suture. Care was taken not to disrupt normal blood flow from the mesenteric vasculature.

After isolating the intestinal segments, polystyrene MSs with a diameter of ~500 nm and 1, 2, and 5 μm were administered locally by direct injection into the jejunum and ileum. The isolated loop was returned to the abdomen, which was closed during the procedure to maintain normal physiologic conditions. After various time points (5 min to 5 h), samples were collected in the following order: portal vein blood (1 mL), celiac arterial blood (1 mL), lungs, heart, spleen, kidneys, liver, isolated loop, rinse from isolated loop, and brain. Given that the total resident time of the rat gastrointestinal (GI) tract is 8–12 h, we determined that 5 h was the most realistic maximum period for a formulation in an intestinal region. All samples were stored at −18 °C until processing. Each experimental condition was repeated four times. We did not perfuse tissues, so distribution to a tissue includes particles that are within the vasculature of the tissue, as well as any particles absorbed into the tissue. The focus of this work was to determine the total uptake across the GI tract, and it would be important to follow up with studies looking at the precise location of particles within tissue. However, this task will be difficult to do quantitatively as perfusion may not remove particles adhered to the endothelium of tissues.

In addition to injecting the MSs into the small intestine, pharmacologic inhibitors were injected into the small intestine to gain a better understanding about which physiologic mechanisms (e.g., endocytosis) facilitate MS uptake. At 0.5, 1, 1.5, 2, and 3 h, CPZ, PMA, CytD, CytB, and colchicine, respectively, were administered. Thirty minutes following administration of the inhibitor, MS suspensions were injected into the intestinal segments. The concentration of polymer following the administration of 500-nm MSs was quantified and compared with animals that did not receive the inhibitors.

Oral Gavage. In addition to administering MSs directly to the jejunum and ileum, 500-nm and 1-μm MSs were fed to animals by oral gavage. Total MS uptake following oral administration was quantified after 5 h. Rats were allowed to recover and had access to standard chow and water ad libitum. During the study, fecal matter and urine were collected. After 5 h, the animal was anesthetized a second time with 3% (vol/vol) isoflurane, and a midline incision was made (identical to the procedure described earlier). Animals that received MSs via oral gavage were killed and had the following samples collected in order: portal vein blood (~1 mL), celiac arterial blood (~1 mL), lungs, heart, spleen, kidneys, liver, stomach, stomach rinse, duodenum, duodenum rinse, jejunum, jejunum rinse, ileum, ileum rinse, cecum, cecum rinse, colon, colon rinse, and brain. The intestinal rinses were combined with their respective sections and were treated as one sample. Additionally, all urine was aspirated from the bladder, and fecal matter was removed from the rectum. Urine and feces were added to urine and fecal samples that were collected throughout the experiment. All samples were stored at −18 °C until further processing. Each experimental condition was repeated four times.

Tissue Processing and Polymer Detection. After killing the animal, gel permeation chromatography (GPC) was used to detect the concentration of polymer within each sample. Excised tissue was minced into small pieces, added to ~5 mL PBS, and homogenized using a Cole-Palmer Ultrasonic Homogenizer CV26 with a high gain Q horn and extender (40% amplitude for 30 s). Homogenized tissue samples were lyophilized for 48 h, leaving behind a powdered tissue digest. Following tissue sample dehydration, polymer was extracted from the tissue by adding chloroform (10 mL), mixing the slurry on an end-over-end mixer for 96 h, and filtering the tissue samples using a 0.1-μm polytetrafluoroethylene (PTFE) syringe filter to remove nonsoluble biological debris. Filtered samples were lyophilized for an additional 24 h and stored at −18 °C. We have validated this method [that was also used by others (9)] by doping tissues with known amounts of polystyrene beads and achieved greater than 90% recovery.

Before sample analysis, the lyophilized powders were reconstituted in 1 mL of chloroform by mixing samples on an end-over-end mixer for 1 h. Each solution was filtered again using a 0.1 μm PTFE syringe filter. Filtered samples were run through a GPC (Shimadzu Corporation) equipped with Styragel HR5E and HR4E columns (Waters Corporation) and a Shimadzu RID-10A refractive index detector. A peak for polystyrene was identified, the area under the curve for various polymer concentrations was calculated, and a linear standard curve was constructed ($R^2 = 0.9993$).

Using the polystyrene calibration curve, the concentration of polystyrene in each lyophilized sample was calculated. Percent uptake was calculated by taking the sum of all quantities of polystyrene detected in each tissue (excluding isolated loop and

loop rinse samples), divided by the total dose administered and multiplying these values by 100. We excluded the rinse sample from this calculation as it represents the portion of the formulation that is not absorbed. Similarly, the isolated loop is also excluded despite the fact that there is absorption [as evidenced by transmission electron microscopy (TEM) and confocal] because the method cannot distinguish absorbed from adsorbed particles. Therefore, this calculation is the most conservative approach to quantify uptake. Inclusion of the isolated loop sample would increase the stated uptake toward a possible overestimate. The biodistribution was compared for each sample across study groups. Additionally, mass balance was measured by dividing the concentration of polymer in each sample by the total administered dose. Positive controls verified that 99.8 ± 1.3% of polystyrene MSs were recovered from tissue samples. No MSs were detected in the negative control samples.

TEM. After completion of the isolated loop experiments, gross anatomical sections of intestine were harvested, washed in warm PBS (37 °C), and fixed in a solution of 20% (vol/vol) paraformaldehyde/20% (vol/vol) glutaraldehyde in sodium cacodylate buffer for 2 h at 37 °C. After fixation, samples were rinsed with sodium cacodylate buffer (0.2 M) and postfixed with 1% osmium tetroxide dissolved in 0.2 M sodium cacodylate buffer for 3 h at room temperature. Immediately following fixation in osmium tetroxide, samples were stained in a solution of 1% uranyl acetate overnight at room temperature. Following fixation and tissue staining, samples were dehydrated using progressively increasing concentrations of ethanol [30–100% (vol/vol)]. Dehydrated samples were embedded and polymerized in hard-grade LR White embedding medium (Electron Microscopy Sciences). Tissue blocks were sectioned to a thickness of 75–85 nm using a Reichert Ultra microtome and diamond knife. Ultrathin sections were placed on copper grids and viewed on a Phillips 410 transmission electron microscope equipped with an Advantage HR CCD camera. Images were acquired with Advanced Microscopy Techniques imaging software.

Confocal Microscopy. Following a 1-h isolated loop experiment, sections of rat jejunum were harvested, washed in PBS, fixed in 75% (vol/vol) formaldehyde for 1 h, and stored at 4 °C until further processing. Before imaging, intestinal sections were stained with FM-143 fluorescent membrane stain (excitation wavelength: 488 nm; emission wavelength: 600 nm) and DAPI fluorescent nuclei stain (excitation wavelength: 358 nm; emission wavelength: 461 nm). The polystyrene MSs were stained with the fluorescent red dye PC-red (excitation wavelength: 377 nm; emission wavelength: 479 nm).

In preparation for imaging, representative intestinal tissue samples were embedded into optimal cutting temperature (OCT) media for sectioning and cut into 20-μm sections with a Leica cryostat. Intestinal tissue samples were imaged using a Leica TCS SP2 AOBS spectral confocal laser scanning microscope using UV excitation (fluorescence emission of 450 nm). Multiple optical sections of each sample were taken. Images were captured, and the resulting images were analyzed using OpenLab software to measure and compare the fluorescence intensity of the tissue samples.

Statistical Analyses. For all experiments, the mean ± SEM is reported. A one-way ANOVA was performed using Microcal Origin Graphical Software. Statistical significance was set at the 0.05 level.

Cytotoxicity of Uptake Inhibitors. To assess the cytotoxicity of uptake inhibitors, a blue-LIVE/DEAD fixable dead cell stain kit from Molecular Probes was used. For each inhibitor (CPZ, PMA, CytB, CytD, and colchicine), an isolated loop with 5.5 h of inhibitor incubation was performed as described above without the administration of MSs. Additionally, a solution of PBS and a 75% (vol/vol) solution of ethanol was used for negative and positive controls, respectively. Following the 5.5-h incubation period, 5 μL of the blue fluorescent reactive dye solution was mixed with 195 μL of phosphate buffer solution, injected into the isolated loop, and incubated for an additional 30 min. The intestinal section was harvested and washed with fresh phosphate buffer solution and placed in 37% (vol/vol) paraformaldehyde for 1 h. Fixed and stained intestinal samples were embedded in OCT media, cut into 50-μm sections with a Leica cryostat, and prepared for confocal microscopy. Samples were imaged on a Leica TCS SP2 AOBS spectral confocal microscope with UV excitation. Emission was read at 450 nm at multiple optical sections. OpenLab software was used to quantitatively compare the relative intensity of staining in all samples.

SI Results and Discussion

As mentioned in the Introduction, no in vivo studies have been published to systematically investigate uptake mechanisms and pathways for the purpose of studying polymeric translocation across the small intestine. Using chemical blockers allows inhibition of specific pathways and, when used in conjunction with quantitative uptake studies, allows investigation of specific pathways. Although the blockers have been chosen for their specificity, each blocker has the potential to be cytotoxic. To ensure that any observed changes in uptake are a result of pathway inhibition, a study was performed to evaluate cytotoxicity. Development of a LIVE/DEAD fluorescent staining assay for in vivo cell viability was used.

The assay described in *SI Materials and Methods* was successful in yielding quantitative results regarding in vivo cell viability. Results are shown in Fig. S2. Representative samples in each study group are shown in blue, corresponding intensity maps are shown in red, and a bar graph of average intensity for each image is shown in the bottom right of Fig. S2. Negative controls of fresh intestinal tissue had a low level of fluorescence intensity (Fig. S2*A*). A small fluorescence signal is expected because intestinal epithelium has a high level of turnover (<24 h) and a basal amount of cell death would be expected.

As a positive control, 70% (vol/vol) ethanol was injected into the intestine. Ethanol induced cytotoxicity, which is evident from the high signal intensity observed in Fig. S2*C*. Additionally, the isolated loop section with ethanol appeared shrunken and had a dark purple to black appearance. This observed change was seen only in tissue that was exposed to ethanol, whereas all other isolated loops included in the study did not undergo any observable changes in appearance. Although the isolated loop technique, and many variations of it, has been implemented for many years, no previous study has investigated cell viability with the technique. In an isolated loop that received a bolus of phosphate buffer solution, a moderate amount of intensity was observed (Fig. S2*B*), indicating that there is an increased amount of cytotoxicity with the isolated loop procedure itself. However, results from the previous chapter illustrated that this level of cytotoxicity does not interfere with the uptake process. Moreover, this can be used as a baseline for the cytotoxicity of the drugs because this is what was experienced in all previous isolated loop studies.

Performing the fluorescent cytotoxicity assay on isolated loops that received pharmacologic blockers demonstrated a low level of toxicity that was comparable to, and never exceeded, the amount of cytotoxicity observed in the isolated loop control (Fig. S2). Therefore, quantitative uptake results gained by the use of these chemical blockers can be considered to be the effect of blocking specific pathways and are not the result of cell toxicity.

1. Okamoto Y, Ninomiya H, Miwa S, Masaki T (2000) Cholesterol oxidation switches the internalization pathway of endothelin receptor type A from caveolae to clathrin-coated pits in Chinese hamster ovary cells. *J Biol Chem* 275(9):6439–6446.
2. Gottlieb TA, Ivanov IE, Adesnik M, Sabatini DD (1993) Actin microfilaments play a critical role in endocytosis at the apical but not the basolateral surface of polarized epithelial cells. *J Cell Biol* 120(3):695–710.
3. Jackman MR, Shurety W, Ellis JA, Luzio JP (1994) Inhibition of apical but not basolateral endocytosis of ricin and folate in Caco-2 cells by cytochalasin D. *J Cell Sci* 107(Pt 9): 2547–2556.
4. Li E, Stupack D, Bokoch GM, Nemerow GR (1998) Adenovirus endocytosis requires actin cytoskeleton reorganization mediated by Rho family GTPases. *J Virol* 72(11): 8806–8812.
5. Said HM (1999) Cellular uptake of biotin: Mechanisms and regulation. *J Nutr* 129(2S Suppl):490S–493S.
6. Song JC, Hrnjez BJ, Farokhzad OC, Matthews JB (1999) PKC-epsilon regulates basolateral endocytosis in human T84 intestinal epithelia: role of F-actin and MARCKS. *Am J Physiol* 277(6 Pt 1):C1239–C1249.
7. Le TL, Joseph SR, Yap AS, Stow JL (2002) Protein kinase C regulates endocytosis and recycling of E-cadherin. *Am J Physiol Cell Physiol* 283(2):C489–C499.
8. Singh RD, et al. (2003) Selective caveolin-1-dependent endocytosis of glycosphingolipids. *Mol Biol Cell* 14(8):3254–3265.
9. Jani P, Halbert GW, Langridge J, Florence AT (1989) The uptake and translocation of latex nanospheres and microspheres after oral administration to rats. *J Pharm Pharmacol* 41(12):809–812.

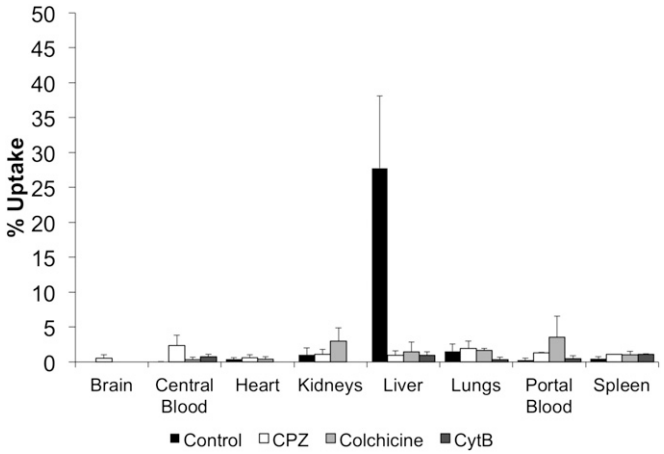

Fig. S1. Biodistribution of 1-μm polystyrene MSs is expressed as a percentage of the total administered dose 5 h after local delivery of to the ileum in the presence of CPZ, colchicine, and CytB and in the absence of drug.

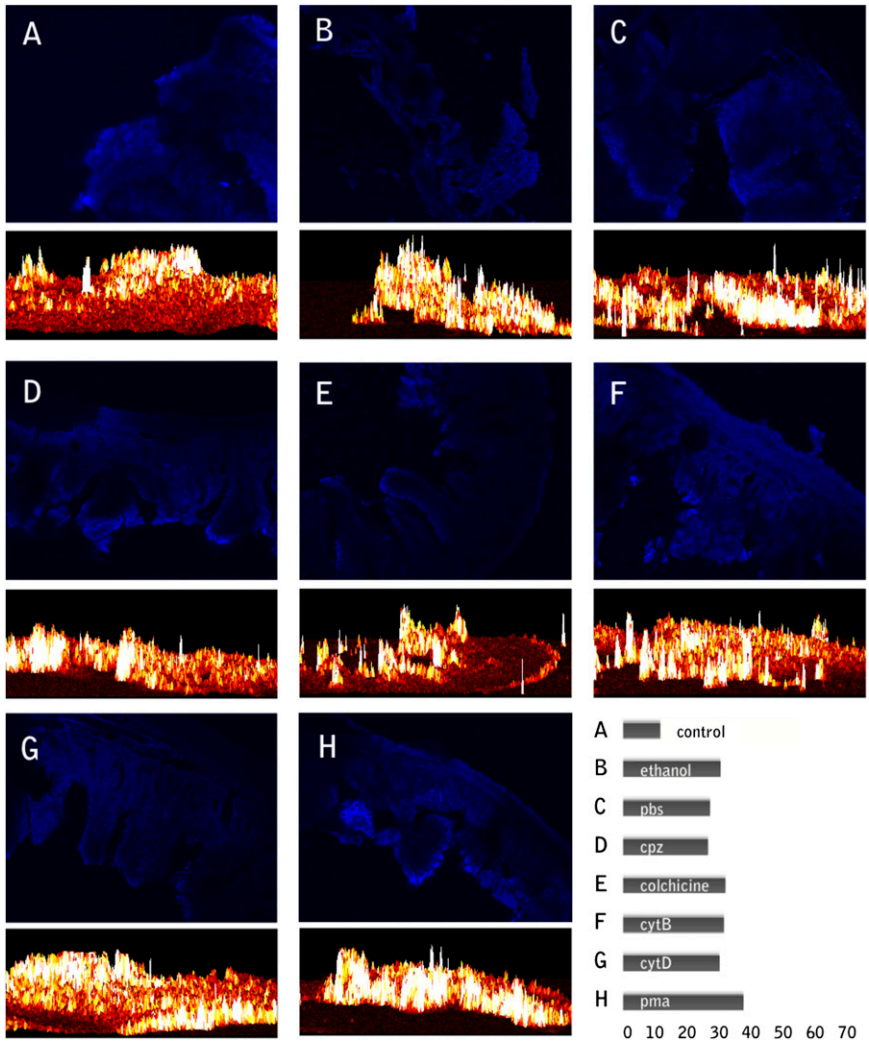

Fig. S2. LIVE/DEAD fluorescent stain was used on isolated intestinal loops 5.5 h after the administration of (*A*) no material (control); (*B*) PBS; (*C*) 70% (vol/vol) ethanol; (*D*) chlorpromazine; (*E*) colchicine; (*F*) CytB; (*G*) CytD; and (*H*) PMA. Intensity maps are shown in red, and the bar graph in the bottom right figure plots the average relative intensities (20 images analyzed for each group; maximum intensity = 255).

Table S1. Biodistribution of particles in specific organs

Organ	500 nm	1 μm	2 μm	5 μm
Brain				
Jejunum	2.40 ± 2.91	0 ± 0	0 ± 0	0 ± 0
Ileum	0 ± 0	0 ± 0	2.09 ± 2.09	0 ± 0
Fed	2.56 ± 2.56	0 ± 0	—	—
Central blood				
Jejunum	0.07 ± 0.05	3.51 ± 3.02	0.09 ± 0.09	0.17 ± 0.09
Ileum	0.86 ± 0.50	0.04 ± 0.03	1.17 ± 0.71	0.10 ± 0.08
Fed	0.07 ± 0.07	0.09 ± 0.09	—	—
Heart				
Jejunum	0.14 ± 0.05	0.87 ± 0.20	0.87 ± 0.54	0.28 ± 0.26
Ileum	3.73 ± 3.03	0.41 ± 0.23	0.12 ± 0.08	0.30 ± 0.18
Fed	0.20 ± 0.12	0.27 ± 0.16	—	—
Kidneys				
Jejunum	3.62 ± 2.69	2.97 ± 1.61	2.82 ± 1.03	0.19 ± 0.19
Ileum	0.35 ± 0.35	1.01 ± 1.01	0.11 ± 0.10	3.98 ± 0.96
Fed	1.80 ± 0.73	1.12 ± 0.65	—	—
Liver				
Jejunum	36.73 ± 11.04	9.01 ± 3.23	11.97 ± 4.06	15.46 ± 5.59
Ileum	26.26 ± 14.20	27.78 ± 10.35	2.12 ± 1.23	7.80 ± 4.02
Fed	22.89 ± 9.81	17.37 ± 7.33	—	—
Lungs				
Jejunum	0.48 ± 0.36	8.49 ± 6.03	0.31 ± 0.25	0.81 ± 0.60
Ileum	0.13 ± 0.08	1.55 ± 0.99	0.51 ± 0.34	0.21 ± 0.21
Fed	0.77 ± 0.56	0.06 ± 0.06	—	—
Portal blood				
Jejunum	2.26 ± 1.31	0.47 ± 0.28	0.24 ± 0.20	0.97 ± 0.60
Ileum	1.63 ± 1.63	0.28 ± 0.28	0.12 ± 0.12	0.11 ± 0.07
Fed	0 ± 0	2.65 ± 1.71	—	—
Spleen				
Jejunum	0.63 ± 0.28	1.24 ± 1.06	0.20 ± 0.16	0.43 ± 0.22
Ileum	3.72 ± 2.62	0.47 ± 0.24	0.16 ± 0.16	0 ± 0
Fed	0.01 ± 0.01	0.05 ± 0.05	—	—

Five hours after administering 500 nm MS, more polymer was detected in the liver than any other region. Larger MS (1, 2, and 5 μm) were also detected in the liver, albeit in smaller quantities. Following local MS administration to the jejunum and ileum, a greater concentration of polymer was detected in the liver, kidneys, and lungs compared to other assayed regions. Polymer was detected in almost every tissue sample, including the brain. MSs with diameters of 2 and 5 μm were delivered locally, but not by oral administration. $n = 4$ animals for each cohort. Data are shown for regions of the rat that were assayed following local delivery to the rat small intestine (jejunum and ileum) or following oral administration (fed). —, not measured.